Research highlight

Rithin Kumar N.B., Vincent Crasta*, B.M. Praveen and Mohan Kumar

Studies on structural, optical and mechanical properties of MWCNTs and ZnO nanoparticles doped PVA nanocomposites

DOI 10.1515/ntrev-2015-0020 Received March 17, 2015; accepted July 27, 2015

Abstract: This paper presents a novel class of multiwalled carbon nanotubes (MWCNTs) and zinc oxide (ZnO) doped polyvinyl alcohol (PVA) nanocomposites prepared using coagulation and solvent casting method. The dopant, ZnO nanoparticles, was prepared using precipitation method, and another dopant, MWCNTs, was treated with H₂SO₄ and HNO₂ taken in 3:1volume ratio to create carboxylated MWC-NTs. Furthermore, prepared ZnO and treated MWCNTs were doped into PVA matrix to prepare PVA nanocomposites by solvent casting technique. The Fourier transform infrared (FTIR) spectra detect the irregular shift in the bands of doped PVA nanocomposites indicating the presence of intra/intermolecular hydrogen bonding creating the interaction between the nanoparticles and neighboring OH group of PVA. Crystallinity of the prepared nanocomposites films was investigated using XRD technique, which explores the average particle size of the embedded nanoparticles and explains the complex formation and variation in crystallinity of the nanocomposites due to interaction of dopants. The decrease in optical energy band gap of nanocomposite films and the information of Urbach energy (E_) were assessed by UV/vis spectroscopy. By using a universal testing machine, the mechanical properties of doped polymer films found escalation for doping percentage concentration x=7.5 wt%. The phase homogeneity, film morphology, and chemical configuration of the nanocomposites were inspected using atomic force microscope, scanning electron microscopy and energy-dispersive X-ray spectroscopy, respectively.

Keywords: dopant; nanocomposites; PVA.

1 Introduction

In recent years, embedding or doping of nanoscopic materials into basic polymeric matrices symbolized a novel substitute to enhance some of the characteristics such as structural, physical, chemical, optical, electrical and mechanical properties of polymer nanocomposites. Thus, incorporation of a small amount of inorganic materials such as metal oxide nanoparticles, carbon nanotubes (CNTs) and clay into the polymer matrix appreciably advances the performance of the polymer materials due to their extraordinary properties and hence finds a lot of applications depending on the dopant materials and concentration [1-5]. Among the various nanomaterials, the application of multiwalled carbon nanotubes (MWCNTs) has been an active research field due to its large flexibility, very high aspect ratio and less mass density. It is indeed these properties of MWCNT that, when incorporated into the polymer matrix, augment the mechanical and electrical properties of polymer nanocomposites. Nowadays, transition metal oxides (TMOs) also play an important role, having applications related to considerable physical and chemical stability, solar cell, high catalysis activity and gas sensors [6, 7]. The purpose of using zinc oxide (ZnO) is due to its direct band gap (E_g=3.37 eV) semiconducting property having large exciton binding energy (60 meV). Out of many TMOs, ZnO is a hopeful material for the various abovementioned applications [8–10]. ZnO, when incorporated into the polymer matrix, significantly enhances its electrical, mechanical as well as optical properties owing to its large interfacial interaction occurring between the organic molecules with inorganic nanoparticles.

Rithin Kumar N.B.: Department of Physics, Srinivas School of Engineering, Mukka, Mangalore, Karnataka, India B.M. Praveen: Department of Chemistry, Srinivas School of Engineering, Mukka, Mangalore, Karnataka, India Mohan Kumar: Department of Mechanical Engineering, Srinivas School of Engineering, Mukka, Mangalore, Karnataka, India

^{*}Corresponding author: Vincent Crasta, Department of Physics, St Joseph Engineering College, Vamanjoor, Mangalore, Karnataka, India, e-mail: vcrasta@yahoo.com

The hydrophilic polyvinyl alcohol (PVA) is chosen as basic polymer matrix due to its versatile properties such as being eco-friendly, semi-crystalline, non-toxic, degradable nature and simple to make thin films with dopants [11–13]. In this study, we used MWCNTs and ZnO doped PVA nanocomposite as a model composite material prepared by simple solvent casting method. Furthermore, these prepared nanocomposites were examined in order to discover the doping effects of CNTs with ZnO on PVA matrix and the doped PVA morphological changes on the polymer crystallinity, tensile properties, optical properties and surface morphology.

2 Materials and methods

2.1 Carboxylated MWCNTs

MWCNTs (75 mg), which were procured from Sigma Aldrich (Germany) (CVD, 95% purity), were allowed to soak in hydrochloric acid (HCl) for 24 h. The dispersed solution obtained from the MWCNTs was poured into 500 ml of distilled water and stirred with magnetic stirrer for 20 min and then filtered using pore 0.1-um Whatman Nylon filter membrane. The achieved residue was washed continuously with distilled water until pH value of the filtrated solution was equal to 7. The obtained MWCNTs were dried in the vacuum oven kept at 600°C for 20 h. The obtained treated MWCNTs were further added in 40 ml of sulfuric acid (H₂SO₄) and nitric acid (HNO₂) taken in 3:1 volume ratio solution and sonicated by using probe ultrasonicator for 2 h. Furthermore, excess distilled water was added to the dispersed solution and filtered using 0.1-um Whatman Nylon filter membrane. The obtained residue was further washed with water several times until the filtrated solution turned neutral. The obtained precursor was dried in the vacuum oven. The amount of the carboxylated MWCNTs obtained (MWCNT-COOH) was 71.8 mg. The reagents HCl, H₂SO₄, HNO₅ are supplied from Merck, India.

2.2 Preparation of ZnO nanoparticles

ZnO nanoparticles for doping purpose were prepared according to Kamellia Nejati et al. [14]. The NaOH and Zn(NO₂)₂.6H₂O chemicals employed in this work were procured from Sigma Aldrich (Germany). Initially, 1-M NaOH solution was prepared by dissolving 40 g of NaOH in 11 of deionized water and heated at 80°C in temperature-controlled magnetic stirrer at 1000 rpm for 1 h until complete

dissolution occurred. Furthermore, 250-ml solution of 0.5 M Zn(NO₂)₂.6H₂O was added to the basic solution, and the reaction mixture was kept stirred at 1000 rpm while the mixture was heated at 80°C for 2 h. The suspended solution formed from the above mixture was separated with a centrifuge to obtain ZnO and washed several times with deionized water until all the traces of NaOH were removed, having neutral pH value. The obtained ZnO was then dried to remove the moisture content at 90°C in an oven for 8 h, and the obtained yield was about 92%. The crystalline structure and morphology of ZnO powder were assessed by XRD and scanning electron microscopy (SEM).

2.3 Preparation of PVA nanocomposite

The basic matrix polymer used is PVA of 97-100 mol% hydrolyzed compound (Mowiol 10-98 fully hydrolyzed grade, Sigma Aldrich, Germany) procured commercially. The procured PVA has molecular weight of $M_w=61,000$ g/mol, degree of polymerization of $P_w=1400$ and bulk density of 0.4-0.6 g cm⁻³. For doping purpose, MWCNTs were procured from Sigma Aldrich (Germany) and WO, nanoparticles were synthesized by precipitation method. The coagulation method was used to produce the PVA/(x)MWCNT (15-x)ZnO nanocomposites. The MWCNTs of x=0%, 1%, 5%, 7.5%, 10%, 14% and 15% weight concentrations were prepared and added to 5 ml of distilled water. Furthermore, each mixer was sonicated by using probe ultra sonicator for 20 min and kept aside. Similarly, ZnO nanoparticles of x=0%, 1%, 5%, 7.5%, 10%, 14% and 15% weight concentrations were prepared and added to 5 ml of distilled water, and each mixer was sonicated by using probe ultra sonicator for 20 min and kept aside. In order to prepare the nanocomposites film, 6 g of solid PVA was dissolved completely in 100 ml of distilled water under constant stirring at 1000 rpm for 1 h while the mixture was heated up to 90°C until the PVA completely dissolved to form a clear viscous solution. The viscous solution was cooled to room temperature while stirring was continued using a mechanical stirrer at 180 rpm for 3 h to ensure homogeneity of the composition. The obtained PVA solution was divided into six equal parts, and each part of viscous solution of prepared PVA was treated by adding mixed fillers PVA/(x) MWCNT(15-x) ZnO, where x=0%, 1%, 5%, 7.5%, 10%, 14% and 15% weight was mixed ultrasonically by probe ultrasonicator for 20 min with pulse on time for 10 s and off time for 10 s. To prepare polymer film of treated polymer, the viscous solution was cast onto a Petri dish and left to dry in air for 3 days at room temperature. The films were peeled off from the casting glass plate and kept in vacuum desiccators for further study. Thus by using dial thickness gauge (Mitutoyo, Japan), the thickness of the prepared polymer composite film was determined. Three trials of thickness were measured at different places of each polymer film, and the average thickness of the film ranging from 100 to 120 µm was obtained.

2.4 Physical measurements

The XRD spectra of the ZnO nanoparticles and PVA nanocomposite films were recorded using a Bruker D8 Advance X-ray diffractometer with Ni filtered, Cu K α radiation of wavelength λ =1.5406 Å, with a graphite monochromator. The scanning was taken in the 2θ range of 10° – 80° with scanning speed of 2°/min. The IR transmittance studies of the PVA nanocomposites were recorded using JASCO FTIR 4100 type A spectrophotometer in the wave number range of 400-4000 cm⁻¹ with a resolution of 4 cm⁻¹. The optical studies of the PVA nanocomposites for various concentration of doping were carried out using JASCO V-630 UV/visible spectrophotometer in the wavelength range of 190-1100 nm. The surface morphological properties of nanocomposites were investigated using JEOL JSM-6380LA SEM and energy-dispersive X-ray spectroscopy (EDS). By using AMETEK LLOYD universal testing machine (LLOYD-5 KN, London, UK), the tensile strength, stiffness, percent elongation (%) and modulus of elasticity of composite were measured. The tests were carried out according to ASTM D-882 standard test (ASTM, 1992) and calculated using NEXYGEN Plus software. The film topography regarding roughness and particle size was analyzed using Bruker (Nano) atomic force microscope (AFM).

3 Results and discussion

3.1 XRD spectra

The XRD spectra of the PVA nanocomposites doped with varied amounts of ZnO and MWCNTs nanoparticles are demonstrated in Figure 1. The intense peaks achieved at $2\theta = 32.33^{\circ}$, 35.15° , 36.93° , 48.49° , 57.66° , 64.23° , 67.67° , 69.35°, 70.46° and 74.29° resemble ZnO nanoparticles (ICSD Collection Code: 154490 and International Center for Diffraction Data, JCPDS 5-0664), and also the small peak found at $2\theta=26.52^{\circ}$ links to MWCNT (JCPDS file no: 48-1449). These obtained peaks confirm the formation

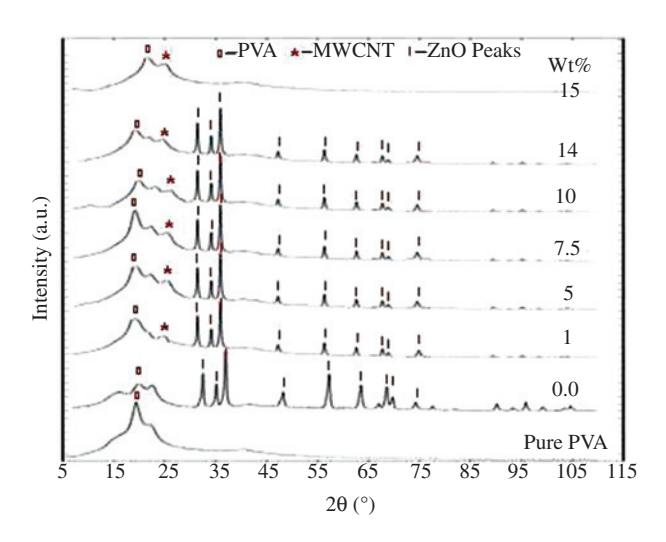


Figure 1: XRD pattern of PVA/(x)MWCNTs(15-x) ZnO for various doping concentration.

of nanocomposites. Additionally, no extra peaks were observed in the spectrum indicating very high purity of ZnO obtained during synthesizing. In case of pure PVA, a broad intense peak observed at scattering angle $(19^{\circ} < 2\theta < 20^{\circ})$ represents the "d" spacing value of 4.57 Å for pure PVA. The occurrence of semi-crystalline nature of PVA is mainly because of the existence of strong intermolecular hydrogen bonding between PVA molecules [15–17]. After doping, the variation in the width of crystalline peaks obtained at the range $2\theta=19^{\circ}<2\theta<22^{\circ}$ implies the changes that occurred in the crystalline phase of PVA matrix. It is observed that the intensity of crystalline peaks of PVA increases up to the dopant concentration x=7.5 wt%. Furthermore, above this concentration, the peaks of PVA shift towards the higher angle, having decrease in intensity, which results in low crystalline phase in PVA matrix. The variation in intensity of crystalline peaks can be attributed to the complex formation of mixed dopants with the PVA molecule. The increase in the intensity of crystalline peaks or particle size is generally due to the interaction between OH groups of PVA with the mixed dopants, causing increase in the intermolecular interaction between PVA chains. The particle size of embedded dopants in PVA matrix is evaluated using Debye formula and presented in Table 1.

Crystallinity plays a considerable role on the physical and mechanical properties of polymer composites. Crystallinity of the polymer is generally determined by using XRD data.

$$%$$
Crystallinity= $\frac{\text{(total area of crystalline peaks)}}{\text{(total area of all peaks)}}$ (1)

Table 1: Structural parameters of the PVA doped with MWCNT's an	id ZnO nanoparticles.
--	-----------------------

Dopants concentrations	(%) Crystallinity	D (nm)	Microstrain(ϵ)×10 ⁻³	δ (10 16 lines/m 2)
Pure PVA	56.64	2.56	13.54	15.258
0 wt%	57.72	35.53	0.975	0.0792
1 wt%	58.22	46.43	0.746	0.0463
5 wt%	63.33	48.95	0.708	0.0417
7.5 wt%	65.81	60.99	0.568	0.0268
10 wt%	64.12	59.86	0.579	0.0279
14 wt%	61.30	38.07	0.910	0.0689
15 wt%	57.34	24.53	1.413	0.1661

Crystallinity of each polymer for different doping concentration is presented in Table 1. This variation in crystallinity entails changes occurred in the structural regularity of the PVA backbone on doping.

The crystallinity behavior of the polymer composites is articulated in terms of relative intensities (I/I_0) , where Iis the intensity in counts at any peaks and I_0 is the intensity of the prominent peak of the crystalline peaks by using PowderX software. The calculated value of relative percentage intensity (I/I_o) is found to be 100 for all the prominent peaks. It can be noticed from Figure 1 that the intensity of the crystalline peak increases around the scattering angle 19° < 2θ < 20° , with an increase in dopant concentration up to x=7.5 wt%, and above x=7.5 wt% doping concentration, the appearance of less intensity peaks starts. The results observed in the XRD spectra illustrate that the embedded dopants interact with PVA molecules forming a complex analogous to that observed in the Fourier transform infrared (FTIR) spectra. The formation of complex is due to dopant ions residing in the interstitial sites of crystalline phase polymer main chains and associates them with hydrogen bond via charge transport processes.

By using first approximation of Debye-Scherrer formula, the crystallite size is evaluated [15].

$$D = \frac{0.9\lambda}{\beta \cos \theta} \tag{2}$$

where λ is the wavelength of X-ray radiation, β is the full width at half-maximum intensity of the peaks and θ is the diffraction angle.

The calculated distance between the hydroxyl groups of crystalline is depicted in Table 1. The increase in crystallinity is due to the increase in average inter crystallite separation, which signifies the strong intermolecular hydrogen bonding leading to the disappearance of molecular motion causing high dense molecular packing in the crystal.

The micro structural strain (ε) is calculated using the following relation [18]:

$$\varepsilon = \beta \cos\theta / 4$$
 (3).

The dislocation density (δ) is evaluated using the formula following [19]:

$$\delta = 1/D^2 \tag{4}.$$

The maximum value of crystallinity is found for the PVA/(x)MWCNT(15-x)ZnO, where x=7.5% weight concentration. The obtained crystal defect parameters such as micro strain and dislocation density show variation with respect to dopant concentration. The variations that occurred are mainly due to the extent of recrystallization process in the polycrystalline films. This implies changes in the structural regularity of the main chains of the polymeric molecules on doping.

3.2 FTIR analysis

FTIR spectral analyses of MWCNTs-COOH, pure PVA and nanoparticles doped PVA nanocomposites were accomplished by KBr pelleting method. The peaks witnessed at 3415 and 1620 cm⁻¹ in the FTIR spectrum (Figure 2) of MWC-NTs-COOH are endorsed to the stretching vibrations of O-H and C=O of carboxyl groups. In addition, the peak at 1080 cm⁻¹ is assigned to the C-O stretching vibration. Occurrence of these peaks in the FTIR spectrum proposes that oxidation of the MWCNTs ensured the presence of COOH groups on the surface of MWCNTs [20, 21]. Furthermore, in Figure 3, the O-H stretching vibration of hydroxyl groups of PVA molecule is specified by a strong broad band at 3623cm⁻¹. The C-H asymmetric stretching vibration absorption bands occur at 2996 and 2920 cm⁻¹ although C-H symmetric stretching vibration is exemplified at 2878, 2850 and 2821 cm⁻¹. The band indicated at 1150.29 cm⁻¹ resembles the C-O stretching of acetyl group, bending deformation with wagging of CH₂ vibrations at 1479.13 cm⁻¹ and C-H wagging witnessed at 1221cm⁻¹ [22, 23]. The FTIR spectrum of doped

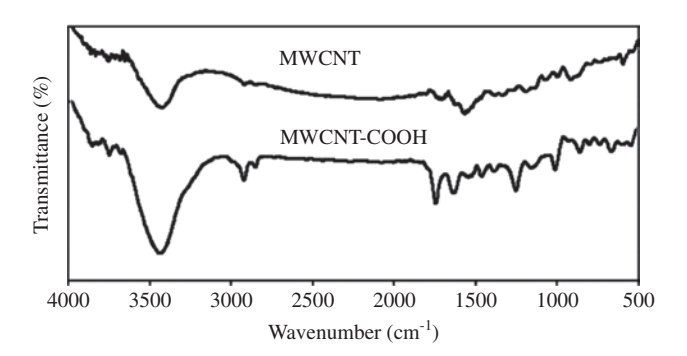


Figure 2: FTIR spectra of pure and functionalized MWCNT.

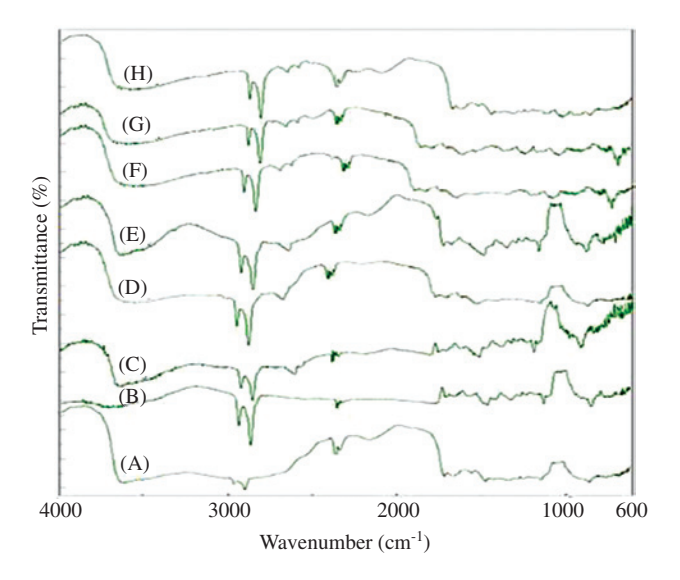


Figure 3: FTIR spectra of PVA/(x)MWCNTs(15-x)ZnO for (A) pure PVA, (B) x=0 wt%, (C) x=1 wt%, (D) x=5 wt%, (E) x=7.5 wt%, (F) x=10 wt%, (G) x=14 wt% and (H) x=15 wt%.

polymer nanocomposites shows an irregular shift in the corresponding bands with a change in intensities. The asymmetrical shifts observed for OH group of PVA nanocomposites shifts from 3624 to 3625 (1 wt%), 3626 (5 wt%), 3627(7.5 wt%), 3625 (10 wt%), 3624 (14 wt%) and 3625 cm⁻¹ (15 wt%) suggest that the interaction of MWCNT and ZnO ions with acetyl group dominates. The irregular shifts in acetyl group (C=O) of PVA nanocomposite shifts from 1641 to 1643 (1 wt%), 1646 (5 wt%), 1648 (7.5 wt%), 1644 (10 wt%), 1642 (14 wt%) and 1640 cm⁻¹ (15 wt%) suggest that the interaction of MWCNT and ZnO ions with acetyl group dominates. The shifts observed in of CH₂ bending vibrations from 1440 to 1441 (1 wt%), 1442 (5 wt%), 1442 (7.5 wt%), 1436 (10 wt%), 1437 (14 wt%) and 1438 cm⁻¹ (15 wt%) suggest the possible chemical interactions of dopant ions with PVA matrix. The changes that occurred in absorption intensity and the irregular shifts are due to hydroxyl groups of the PVA chain gifted to forming more or less stable complex chemical composites interrelated with nanoparticles. These observations give evidence regarding the interaction of PVA molecule with nanoparticles. Apart from these, the rise in novel bands may be due to the creation of defects induced by charge transfer reaction occurring between PVA main chains with the nanoparticles dopant. These elucidations endorsed that the inter/intramolecular interaction between MWCNTs and ZnO ions with PVA acetyl group dominates. The chemical interactions occurring between Zn and MWCNT ions with PVA chain can be specified by the shift in bending of CH. vibrations. The occurrence of chemical interaction is also supported by the shift in frequency of acetyle C-O stretching of PVA. These interpretations and observations lead to a conclusion that the formation of complex configuration between PVA molecules and mixed nanodopants occurred via intra/intermolecular hydrogen bonding.

3.3 UV/visible spectral analysis

Figure 4 represents the recorded absorbance spectra of pure PVA and doped PVA films for different dopant concentrations. As the doping concentration increases until x=7.5 wt%, the optical absorption of the composite film increases. Increased doping concentration more than x=7.5 wt% results in lower optical absorption of the composite films. The absorption peaks for pure PVA are found at 350.5 nm, and as the doping concentration increases up to x=7.5 wt%, the wavelength of absorption peaks increases. For x=7.5 wt% concentration, the absorption wavelength was found at a maximum of 382.1 nm and

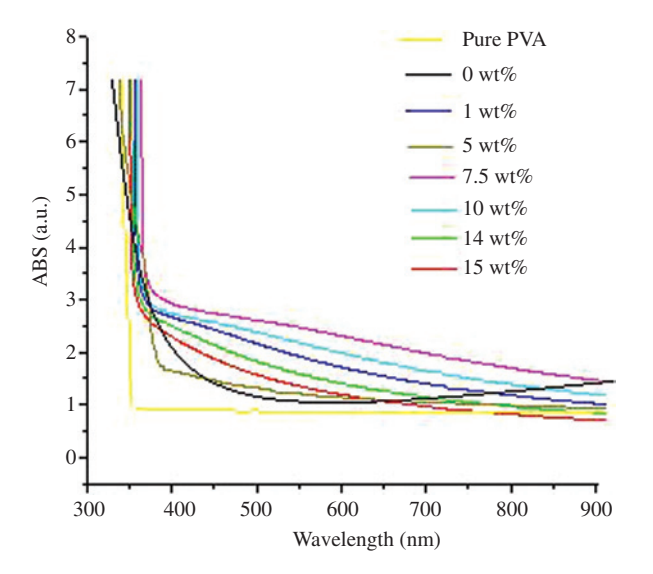


Figure 4: UV/visible spectra of PVA/(x)MWCNTs(15-x)ZnO nanocomposites for various doping concentration.

further increase in doping concentration wavelength of absorption spectra found a decreasing trend. These shifts occurring in the absorption band represent the existence of hydrogen bonding between the adjacent OH groups of the PVA with the mixed dopant ions. Hence, it is very clear from Figure 4 that the spectra have high absorbance in the near ultraviolet regions and low absorbance in the visible and near infrared regions. These observations can be explained based on Beer's law that the absorption of radiation is directly proportional to the number of absorbing molecules in the sample. The shift observed in the absorption edge of the doped PVA composites is mainly due to variation in crystalline parameters, which in turn changes the energy band gap. The variation of the absorption coefficient, α , as a function photon energy was calculated from equation (5):

$$\alpha = \frac{2.303A}{d} \tag{5}$$

where *A* is the absorbance and *d* is the thickness of sample. From the UV/visible spectra, the optical energy band gap is assessed by transforming the absorption spectrum in to Tauc's plot by means of the frequency-dependent absorption coefficient given by Mott and Devis [24, 25]:

$$\alpha(\nu) = \frac{\beta (\text{hv-}E_g)^r}{\text{hv}}$$
 (6)

where β is a constant and the exponent r is an empirical index, which is equal to 2 for indirect allowed transition in the quantum mechanical sense, responsible for optical absorption.

The linear behavior witnessed in the graph plotting $(\alpha h v)^{0.5}$ vs. the photon energy hv at room temperature gives a confirmation for indirect allowed transition. Extrapolation of the linear portion of the obtained curve to a point $(\alpha h v)^{0.5}$ =0 provides the optical energy band gap E_{α} for the doped PVA nanocomposite films (Figure 5). The occurrence and deviation observed in the optical energy gap E are attributed to arouse the complex formation through intra/intermolecular hydrogen bonding. These complex interactions significantly change the microstructural variation within the polymer matrix. This microstructural variation is reflected in the form of varying band gap E_a with respect to the dopant concentrations as shown in Figure 6. The occurrence of the crystalline or amorphous nature of the polymer film is also assessed by optical absorption data. Furthermore, for longer wavelength in the spectrum (low absorption levels), the absorption coefficient $\alpha(v)$ is described by the Urbach exponential law [26]. The Urbach energy is related to the absorption co-efficient as

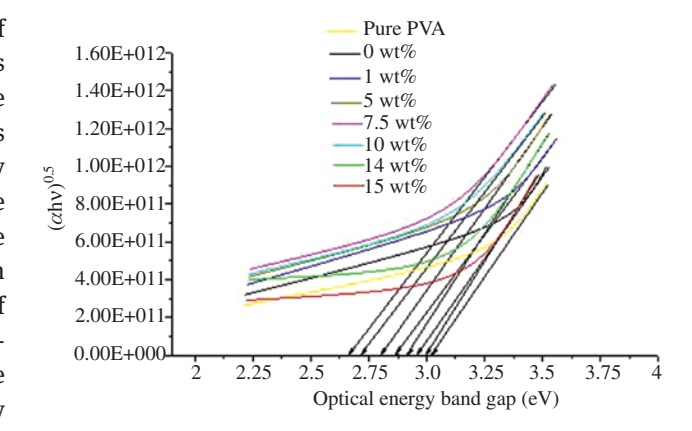


Figure 5: Optical energy band gap PVA/(x)MWCNTs(15-x)ZnO for various doping concentration.

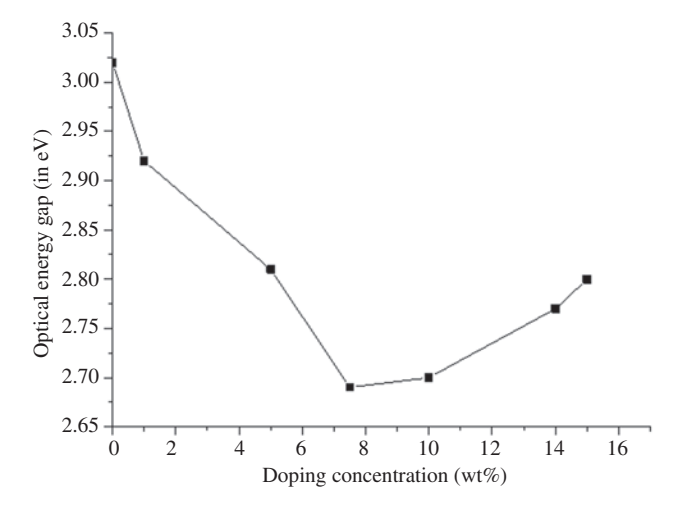


Figure 6: Variation of optical energy gap with doping concentration.

$$\alpha(hv) = \alpha_0 \exp\left(\frac{hv}{E_u}\right) \tag{7}$$

where $\alpha_{\rm 0}$ is a constant dependent on the optical band gap but independent of photon energy hv and $\rm E_u$ is called Urbach energy.

Generally, the Urbach energy E_u is the measure of disorder in the system typically interpreted by the width of the tail in localized states of the forbidden band gap. Experimentally, the absorption coefficient $\alpha(v)$ close to the band edge gives an idea about an exponential dependence on photon energy (hv) and obeying Urbach's rule. The Urbach energy of different doping concentration is evaluated by fitting the linear region of figure by the method of least square to the straight line equation $(\ln \alpha = hv/E_u + Constant)$, and the assessed values of E_u are presented in Table 2. A monotonic behavior of E_u on the

Table 2: The variation of Urbach energies of PVA doped with different doping concentration of nanoparticles.

Sl No.	Doping concentration (wt%)	Urbach energy (eV)	
1	Pure PVA	2.47	
2	0	7.96	
3	1	8.45	
4	5	8.99	
5	7.5	9.75	
6	10	9.03	
7	14	8.65	
8	15	7.53	

increase of dopant concentration is observed. It is very clear from Table 2 that with the increase in dopant concentration, Urbach energy E, found increasing trend up to x=7.5 wt% and then decreased with further increase in dopant concentration. The variation of E_ in nanocomposite films is endorsed by the mobility concept as proposed by Davis and Mott [24]. This behavior is mainly due to the introduction of point defects induced by nanodopants dispersed in the polymer matrix. Thus, the increase in dopant concentration creates additional defects causing increase in density of localized states. The variations in dopant concentration results in defects causing localized states to overlap and extend to the mobility gap. This overlap generally changes the Urbach energy E, of the polymeric nanocomposites. Thus, the values of E, obtained interpret that the polymer composites are crystalline in nature. Likewise, occurrence of sharp XRD peaks also confirms the crystalline nature of polymer composites.

3.4 Mechanical properties

The mechanical properties such as tensile properties, Young's modulus, etc. of doped polymeric nanocomposite materials were carried out using universal testing machine at room temperature in air. The effect of the MWCNTs and ZnO deploys the tensile strength, Young's modulus and percentage elongation at facture of the PVA/(x)MWCNT(15-x)ZnO nanocomposite films, as shown in Table 3. It is obvious that the addition of mixed dopants MWCNTs and ZnO significantly increased the tensile strength and modulus from 0 to 7.5 wt% and then dropped. This result indicates that the addition of MWCNTs/ZnO into the PVA matrix results in strong interactions between the polymer matrix and mixed fillers, thereby restricting the matrix motion and promoting rigidity. Generally, due to an inverse Hall-Petch effect at lower grain size, it limits the dislocations bowing out between the obstacles without touching a boundary, and there is no enough space for pile-ups to form. This leads to the decrease in percentage elongation at facture [27, 28]. Further addition of dopant concentration for x>7.5 wt% decreases the tensile strength and modulus but remained greater than the original PVA film. This reduction is due to inter-particle interactions, which lead to the creation of weak points. Moreover, the increase in degree of crystallinity and the morphological behavior of the crystalline material also have significant effects on the mechanical properties of polymers. This in turn has profound effect on the tensile strength of the polymer. It can be noted from

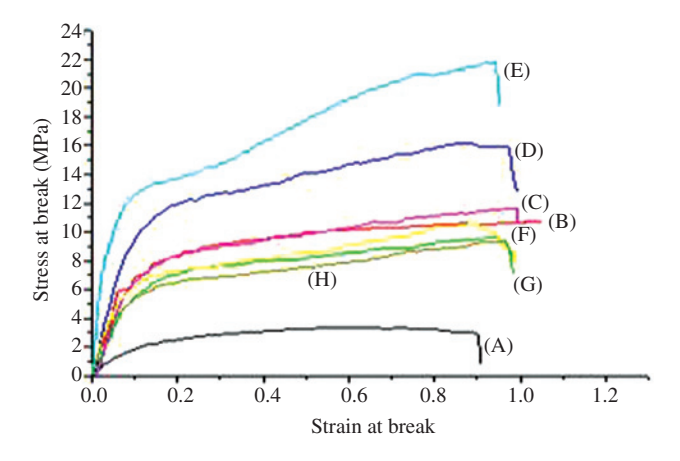


Figure 7: Stress-strain curves of PVA/(x)MWCNTs(15-x)ZnO with (A) pure PVA, (B) x=0 wt%, (C) x=1 wt%, (D) x=5 wt%, (E) x=7.5 wt%, (F) x=10 wt%, (G) x=14 wt% and (H) x=15 wt%.

Table 3: Tensile properties of pure and doped PVA films.

Sl No.	Sample (wt%)	Tensile strength (MPa)	Stiffness (kN/m)	Young's modulus (MPa)	Percentage total elongation at fracture
1	Pure PVA	2.901	5.3490	45.330	92.53
2	0	11.14	9.8261	196.523	107.34
3	1	11.87	9.9059	198.658	100.21
4	5	16.04	10.3994	200.45	96.85
5	7.5	21.82	11.3474	214.267	94.45
6	10	10.575	10.1376	194.864	99.15
7	14	9.934	8.8816	196.523	97.47
8	15	9.544	9.7478	200.51	95.25

Figure 7 that the elongation at break gradually decreases from 0 to 7.5 wt% of mixed filler loading. This phenomenon can be enlightened by the occurrence of strong interaction between the filler-matrix interactions.

3.5 SEM and EDS studies

Figure 8 represents the surface micrographs of doped polymer nanocomposites at room temperature (31°C). The surface morphology of PVA/(x)MWCNT(15-x)ZnO was found almost smooth, and the nanoparticles were distributed homogenously on the surface. The particle size measured in the SEM images of the nanocomposite film was found analogous to the particle size measured using the XRD spectra data owing to grain size from 30 nm to 59 nm. The SEM image (Figure 8) is taken at a magnification of

 $3000\times$, and at more than $3000\times$, cracks started to appear in the image. The particles more than 30 nm refer to ZnO, and those below 20 nm size refer to MWCNTs, which are analogous to the calculated particle size of the dopants using XRD spectra before doping process.

Table 4: Percentage distribution of ZnO and MWCNTs nanoparticles in the PVA composites film.

ZAF Method standardless quantitative analysis Fitting coefficient: 0.3711						
СК	0.277	57.45	0.14	66.28	58.8242	
O K	0.525	37.76	0.69	32.70	33.2246	
Zn K	8.630	4.79	1.94	1.02	7.9512	
Total		100.00		100.00		

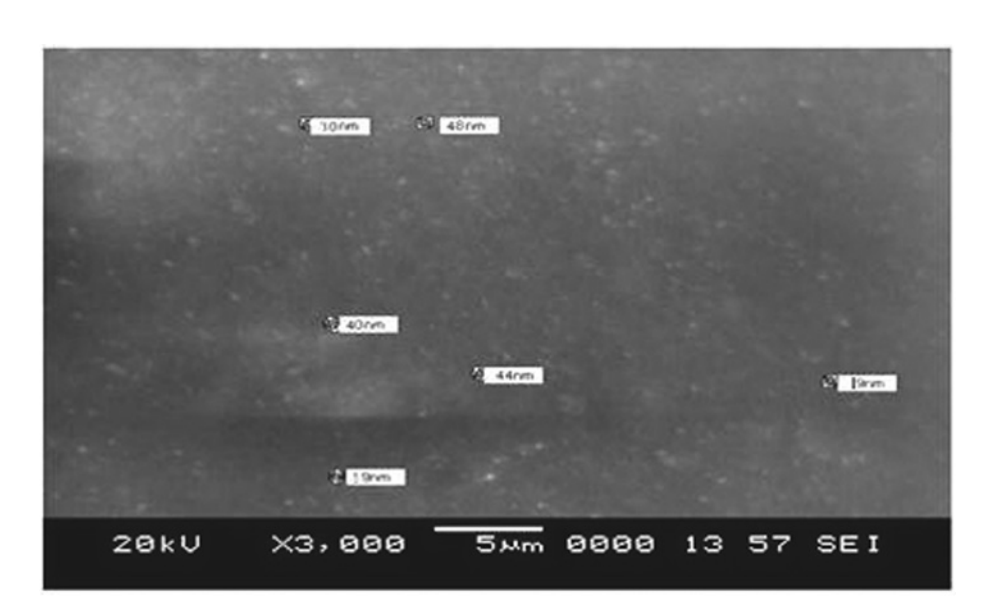


Figure 8: SEM images of PVA/(x)MWCNTs(15-x)ZnO, where x=7.5% weight polymer nanocomposite.

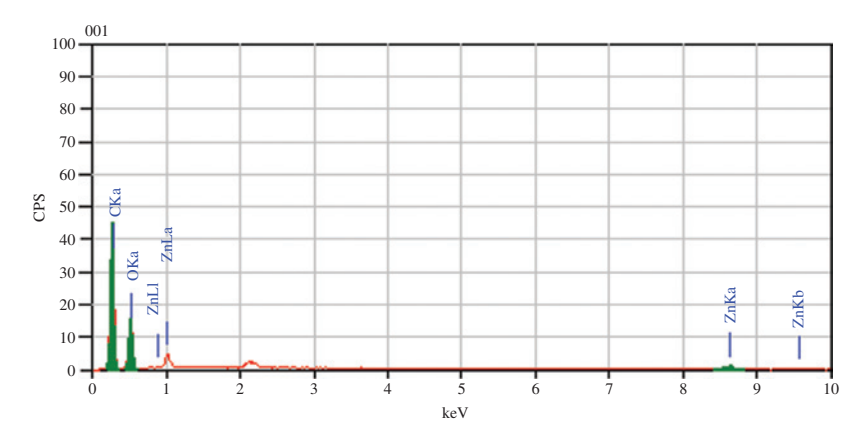


Figure 9: Distribution of nanosized MWCNT's and ZnO dopants in the composite film.

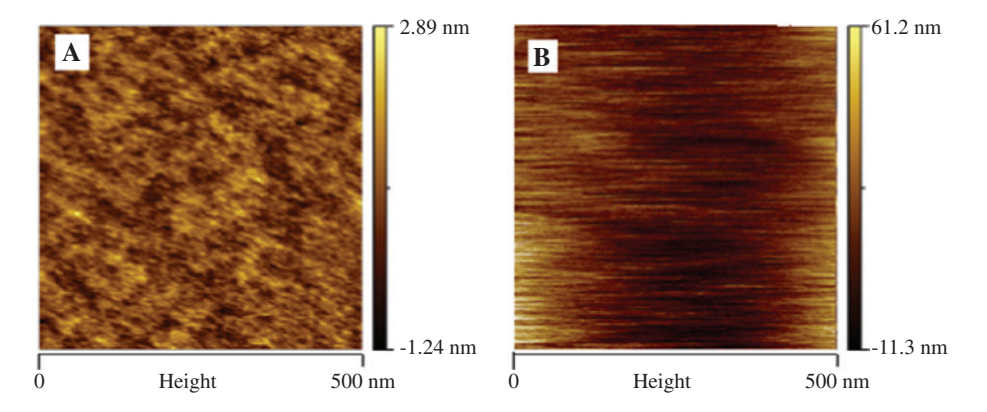


Figure 10: AFM two-dimensional images of (A) pure PVA and (B) doped PVA.

In order to inspect the elemental composition and homogenous distribution of ZnO and MWCNT nanoparticles in PVA polymer composite films, EDS is accomplished. The prepared PVA nanocomposite films were primarily sputtered by using gold particles to resist the artifacts created above the film surface because of charging. Figure 9 signifies the uniform distribution of nanoparticle ZnO and MWCNTs dopants in PVA matrix and confirms the presence of ZnO and MWCNTs in the film. As it is a composite, the dispersion of small amount of doping in the large PVA film may reduce the total CPS by <100%. The percentage distribution of nanosized ZnO and MWCNTs dopants in the PVA composite film is specified in Table 4.

3.6 Film topography

Figure 10A and B shows the two-dimensional images of an undoped and doped PVA nanocomposites, whereas

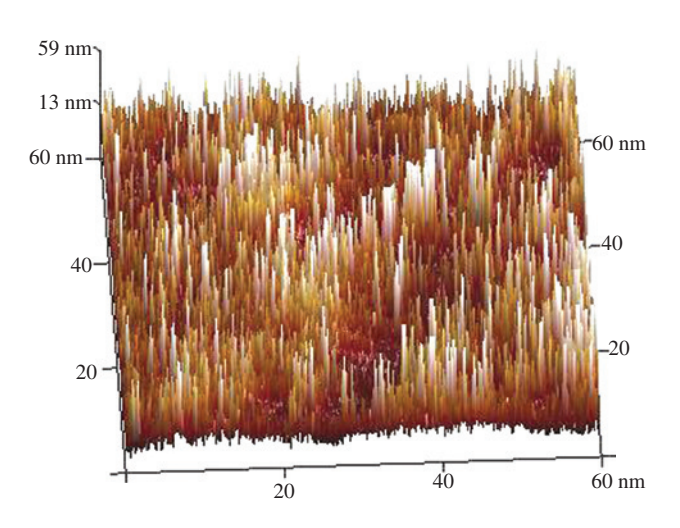


Figure 11: AFM three-dimensional images of nanoparticles doped PVA nanocomposite.

Figure 11 epitomizes the three-dimensional AFM image of doped polymer composites. It is very clear from the AFM images that the pure film has smooth surface and smaller grain size. Furthermore, doping the film with nanoparticles alters the grain size and roughens the surface of the composites. The variation in root mean square value of surface with respect to the dopant concentration is observed, causing variation in the crystallinity of the film.

4 Conclusions

The results obtained with the investigated PVA doped with MWCNTs and ZnO polymer nanocomposites prepared by coagulation mixing and solution casting method allow us to draw the following conclusions:

- The XRD results demonstrate the increase in crystallinity up to 7.5 wt% concentration, indicating the strong inter/intramolecular hydrogen bonding with complex formation, which disappears with the molecular motion causing compact molecular packing.
- The FTIR study shows that the MWCNTs and ZnO ions of the dopant interact with the OH groups of PVA backbone and form a complex via intra/intermolecular hydrogen bonding.
- The UV/vis spectra show drastic decrease in optical energy band gap (E_c) with the increase in dopant concentration up to 7.5 wt%.
- Urbach energy (E_n) found an increasing trend up to x=7.5 wt% and then decreased with the further increase in dopant concentration, creating additional defects causing increase in density of localized states.
- The mechanical studies indicate that the addition of the MWCNTs and ZnO nanoparticles in PVA matrix with weight percentage concentration x=7.5 wt% increases the tensile strength and Young's modulus

- whereas decreases the percentage elongation at facture.
- The SEM and EDAX data indicate that the distribution of nanosized MWCNTs and ZnO dopants is uniform and confirms the presence of nanoparticles in the film.
- AFM images reveal the variation in root mean square value of surface with respect to the dopant concentration, causing variation in the crystallinity of the film.

References

- [1] Wang ZL, Kong XY, Ding Y, Gao P, Hughes WL. Semiconducting and piezoelectric oxide nanostructures induced by polar surfaces. Adv. Funct. Mater. 2004, 14, 943-956.
- [2] Huang YH, Zang Y, Liu L, Fan SS, Wei Y, He J. Controlled synthesis and field emission properties of ZnO nanostructures with different morphologies. J. Nanosci. Nanotechnol. 2006, 6, 787-790.
- [3] Jariwala D, Sangwan VK, Lauhon LJ, Marks TJ, Hersam MC. Carbon nanomaterials for electronics, optoelectronics, photovoltaics, and sensing. Chem. Soc. Rev. 2013, 42, 2824-2860.
- [4] Peng C, Zhang S, Jewell D, ChenG Z. Carbon nanotube and conducting polymer composites for supercapacitors. Prog. Nat. Sci. 2008, 18, 777-788.
- [5] Huang F, Vanhaecke E, Chen D. In situ polymerization and characterizations of polyaniline on MWCNT powders and aligned MWCNT films. Catal. Today 2010, 150, 71-76.
- [6] Wang ZL. Zinc oxide nanostructures: growth properties and applications. J. Phys. Condens. Matter. 2004, 16, 829-858.
- [7] Suchea M, Christoulakis S, Moschovis K, Katsarakis N, Kiriakidis G. ZnO transparent thin films for gas sensor applications. Thin Solid Films. 2006, 515, 551-554.
- [8] Michalet X, Pinaud FF, Bentolila LA, Tsay JM, Doose S, Li JJ, Sundaresan G, Wu AM, Gambhir SS, Weiss S. Quantum dots for live cells, in vivo imaging, and diagnostics. Science 2005, 307, 538-544.
- [9] Wilson WL, Szajowski PF, Brus LE. Quantum confinement in size-selected, surface-oxidized silicon nanocrystals. Science 1993, 262, 1242-1244.
- [10] Ding Z, Quinn BM, Haram SK, Pell LE, Korgel BA, Bard AJ. Electrochemistry and electro generated chemiluminescence from silicon nanocrystal quantum dots. Science 2002, 296, 1293-1297.
- [11] Tang Z, Wang Y, Podsiadlo P, Kotov NA. Biomedical applications of layer-by-layer assembly: from biomimetics to tissue engineering. Adv. Mater. 2006, 18, 3203-3224.
- [12] Fujigaya T, Morimoto T, Nakashima N. Isolated single-walled carbon nanotubes in a gel as a molecular reservoir and its

- application to controlled drug release triggered by near-IR laser irradiation. Soft Matter. 2011, 7, 2647-2652.
- [13] Chen T, Cai Z, Qiu L, Li H, Ren J, Lin H, Yang Z, Sun X, Peng H. Synthesis of aligned carbon nanotube composite fibers with high performances by electrochemical deposition. J. Mater. Chem. A 2013, 1, 2211-2216.
- [14] Nejati K, Rezvani Z, Pakizevand R. Synthesis of ZnO nanoparticlesand investigation of the ionic template effect on their size and shape. Int. Nano Lett. 2011, 1, 75-81.
- [15] Zidan H M. Structural properties of CrF₂, and MnCl₂-filled poly(vinyl alcohol) films. J. Appl. Polym. Sci. 2003, 88, 1115-1120.
- [16] Bhajantri RF, Ravindrachary V, Harisha A, Crasta V, Suresh Nayak P, Poojary B. Microstructural studies on BaCl2 doped poly(vinyl alcohol). Polymer 2006, 47, 3591-3598.
- [17] Rithin Kumar NB, Crasta V, Bhaiantri RF, Prayeen BM, Microstructural and mechanical studies of PVA doped with ZnO and WO₃ composites films. J. Polym. 2014, 2014, 1-7.
- [18] Williamson GB, Smallman RC. Dislocation densities in some annealed and cold-worked metals from measurements on the X-ray Debye-Scherrer spectrum. Phil. Mag. 1956, 1, 34-46.
- [19] Kundu PP, Biswas J, Kim H, Choe S. Influence of film preparation procedures on the crystallinity, morphology and mechanical properties of LLDPE films. Eur. Polym. J. 2003, 39, 1585-1593.
- [20] Vukovic GD, Marinkovic AD. Removal of cadmium from aqueous solutions by oxidized and ethylene- diamine-functionalized multi-walled carbon nanotubes. Chem. Eng. J. 2011, 15, 238-248.
- [21] Vukovic GD, Marinkovic AD, Skapin SD. Removal of Pb(II) from aqueous solution by amino multi walled carbon nanotubes. Chem. Eng. J. 2011, 3, 855-865.
- [22] Soliman Selim M, Seoudi R, Shabaka AA. Polymer based films embedded with high content of ZnSe nanoparticles. Mater Lett. 2005, 59, 2650-2654.
- [23] Shin EJ, Lee YH, Choi SC. Study on the structure and processibility of the iodinated poly(vinylalcohol). I. Thermal analyses of iodinated poly(vinyl alcohol) films. J. Appl. Polym. Sci. 2004, 91,
- [24] Mott NF, Devis EA. Electronic Process in Non-crystalline Materials. 2nd ed., Oxford University Press: Oxford, UK, 1979.
- [25] Mott NF. Conduction in Non-Crystalline Materials. 2nd ed., Calrendon Press: Oxford, UK, 1993.
- [26] Urbach F. The long-wavelength edge of photographic sensitivity and of the electronic absorption of solids. Phys. Rev. 1953,
- [27] Hall EO, Petch NJ. The cleavage strength of crystals. J. Iron Steel Inst. 1953, 174, 25-28.
- [28] Kumar KS, Van Swygenhoven H, Suresh S. Mechanical behavior of nanocrystalline metals and alloys. Acta Mater. 2003, 51, 5743-5774.

Bionotes



Rithin Kumar N.B. Department of Physics, Srinivas School of Engineering, Mukka, Mangalore, Karnataka, India

Rithin Kumar N.B. is pursuing his PhD degree in the area of polymer nanocomposites at St Joseph Engineering College, Vamanjoor, Mangalore, under the Visvesvaraya Technological University, Belgaum, Karnataka. He is an Assistant Professor at the Department of Physics, Srinivas School of Engineering, Mukka, Mangalore. His research fields of interest are composite materials, thin films, nanomaterials and polymer nanocomposites. Kumar has published many research articles in the areas of composite materials, nanomaterials and polymer nanocomposites in various peer-reviewed international journals and conferences.



Vincent Crasta Department of Physics, St Joseph Engineering College, Vamanjoor, Mangalore, Karnataka, India, vcrasta@yahoo.com

Vincent Crasta holds MSc and PhD degrees from Mangalore University, Mangalore, Karnataka. He is Professor and Head of the Department of Physics, St Joseph Engineering College, Vamanjoor, Mangalore. He has 20 years' experience in teaching and research. He has published and presented more than 40 research papers in international and national journals and at conferences and has received several grants from funding agencies including Board of Research in Nuclear Sciences (BRNS), India, etc. Currently, five research scholars are doing research under his supervision. His areas of research interest are single crystals, NLO materials, polymer nanocomposites and nanomaterials.



B.M. Praveen Department of Chemistry, Srinivas School of Engineering, Mukka, Mangalore, Karnataka, India

B.M. Praveen works as an Associate Professor in and Head of the Department of Chemistry in Srinivas School of Engineering, Mukka, Mangalore. His areas of research include corrosion studies, nanomaterials, nanocomposites, etc. Currently, five research scholars are doing research under his supervision. He has coauthored numerous highly cited journal publications, conference articles and book chapters in the aforementioned topics and has received several awards and grants from various funding agencies including Department of Science and Technology (DST), India, Vision Group of Science and Technology (VGST), India and All India Council for Technical Education-Modernization and Removal of Obsolescence (AICTE-MDROBS).



Mohan Kumar Department of Mechanical Engineering, Srinivas School of Engineering, Mukka, Mangalore, Karnataka, India

Mohan Kumar has been working as an Assistant Professor at the Department of Mechanical Engineering, Srinivas School of Engineering, Mangalore, for the past 5 years. He has a 12 years' experience in teaching and 2 years' industry. He has authored one text book and presented many papers at national and international conferences. He has also published many papers in international journals. His fields of interest are vibrations, design, nanomaterials and composite materials.